

A Numerical Model for the Virtual Calibration of a Highly Efficient Spark Ignition Engine

Original

A Numerical Model for the Virtual Calibration of a Highly Efficient Spark Ignition Engine / Rolando, L., Millo, F., Castellano, G., Tahtouh, T., Andre, M., Bocchieri, F.. - In: SAE TECHNICAL PAPER. - ISSN 0148-7191. - ELETTRONICO. - 1:(2023). (2023 JSAE/SAE Powertrains, Energy & Lubricants International Meeting KYOTO 29 Agosto - 1 Settembre 2023) [10.4271/2023-32-0059].

Availability:

This version is available at: 11583/2984509 since: 2025-11-28T10:10:13Z

Publisher:

SAE

Published

DOI:10.4271/2023-32-0059

Terms of use:

This article is made available under terms and conditions as specified in the corresponding bibliographic description in the repository

Publisher copyright

(Article begins on next page)

A Numerical Model for the Virtual Calibration of a Highly Efficient Spark Ignition Engine

Luciano ROLANDO, Federico MILLO, Giuseppe CASTELLANO
Politecnico di Torino

Toni TAHTOUH, Mathieu ANDRE
IFP Energies nouvelles I.Carnot IFPEN TE

Francesco BOCCHIERI
FEV Italia s.r.l.

Copyright © 2023 SAE Japan and Copyright © 2023 SAE International

ABSTRACT

Nowadays numerical simulations play a major role in the development of future sustainable powertrain thanks to their capability of investigating a wide spectrum of innovative technologies with times and costs significantly lower than a campaign of experimental tests. In such a framework, this paper aims to assess the predictive capabilities of an 1D-CFD engine model developed to support the design and the calibration of the innovative highly efficient spark ignition engine of the PHOENICE (PHEV towards zero Emissions & ultimate ICE efficiency) EU H2020 project. As a matter of fact, the availability of a reliable simulation platform is crucial to achieve the project target of 47% peak indicated efficiency, by synergistically exploiting the combination of innovative in-cylinder charge motion, Miller cycle with high compression ratio, lean mixture with cooled Exhaust Gas Recirculation (EGR) and electrified turbocharger. Since the engine is expected to operate in highly diluted conditions, particular attention was paid to the definition of a reliable combustion model to accurately predict the burn duration and the occurrence of abnormal combustion phenomena. A preliminary set of experimental data measured at 3000 RPM and 7 bar BMEP, including both EGR and λ variations, was used to assess the predictive capabilities of the model. Afterwards, the developed virtual test rig was exploited to perform a calibration of the engine in terms of optimal λ and EGR combinations and the results obtained for two operating points, a low load 1500 RPM and 5.5 bar BMEP and a high load 3000 RPM and 13 bar BMEP, were presented and discussed. Findings showed that best efficiency values, well above 40% indicated efficiency, could be obtained with moderate dilution and EGR rates thanks to knock suppression capability for the high load point and de-throttling for the low load point.

INTRODUCTION

The Fit-for-55 package recently introduced by the European Commission [1] mainly relies on powertrain electrification to completely decarbonize the on-road transport sector. Nevertheless, a recent study of the FVV [2] demonstrates that the speed of deploying carbon neutral solutions is much more important than technology selection to achieve a rapid transition toward a sustainable mobility. As a result, in the framework of a diversification of energy carriers, the development of a new generation of environmentally friendly Internal Combustion Engines (ICEs) can still represent a promising path to meet the future Green House Gases (GHG) emission reduction targets.

Within this track, the PHOENICE (PHEV towards zero Emissions & ultimate ICE efficiency) EU H2020 project [3] aims at developing a C SUV-class Plug-in Hybrid Electric Vehicle (PHEV) demonstrator capable of achieving a 10% fuel consumption reduction compared to the "baseline" EU6 vehicle, currently on the market, while being fully compliant with the recently announced new EU7 pollutant emissions limits [4], as summarized in [Table 1](#) and [Table 2](#), respectively.

Table 1: Vehicle and engine efficiency targets

Fuel Consumption	-10% vs Baseline Vehicle (CS WLTC Test)
ICE Efficiency	47% Peak Gross Indicated Efficiency

Table 2: Pollutant emissions targets (RDE)

CO	400 mg/km	CH₄	10 mg/km
NMOG	25 mg/km	HCOH	5 mg/km
NO_x	20 mg/km	N₂O	10 mg/km
PM	2 mg/km	NH₃	10 mg/km
PN (>10nm)	5 × 10 ¹⁰ #/km		

The achievement of such ambitious targets requires the use of innovative engine technologies capable to raise the peak indicated efficiency beyond 45% [5]. Among these, the ultra-lean combustion concept stands out as one of the most promising thanks to the decreased cooling and exhaust energy losses caused by the reduction of the combustion temperature. Further increases in engine efficiency can be achieved by increasing the compression ratio and improving the combustion phasing, both of which are made possible by the lower knock likelihood of lean-burn operation [6, 7]. On the other side, technologies such as Turbulent Jet Ignition (TJI) [8] or advanced in-cylinder charge motions [9] appear to be essential to enhance the turbulence levels and the combustion speed to limit the cycle-to-cycle variability and to extend the lean operating region [10]. Exhaust Gas Recirculation (EGR) represents another valuable solution for charge dilution. As a matter of fact, it can be employed not only at high load to prevent knock [11, 12], but also at part load where the reduction in volumetric efficiency caused by the inert gas recirculation allows engine de-throttling and, consequently, a reduction in pumping losses [13]. Further efficiency enhancements can also be achieved through Variable Valve Actuation (VVA) systems. As it turns out, the capability to completely control the valve lift profile not only permits part-load engine operation without any throttling, but also, thanks to engine cycle Millerization and the resulting knock reduction, enables an increase in the engine compression ratio. [14, 15]. In addition to the combustion system improvement, the integration of advanced turbocharging technologies [16] in a hybrid powertrain architecture can further contribute to the overall efficiency enhancement. As a matter of fact, electric turbochargers can guarantee the necessary boost pressure in all operating conditions, to reduce turbo-lag phenomena during transient maneuvers and to recover waste enthalpy from exhaust gases whenever possible [17].

Despite their huge potential, the combined use of these technologies leads to an increase of the powertrain complexity, which can only be effectively handled through the synergic combination of numerical simulations and experimental testing. In such a framework, 0/1D CFD platforms can be extremely useful for supporting both the early stages of the design processes, by investigating a wide variety of configurations in a limited amount of time [18], as well as for the successive engine calibration. These potentialities allow to identify in an easier way possible synergy among the above-mentioned

technologies and to optimize the engine calibration parameters with a reduced number of experimental tests.

In this context, this paper assesses the capability of a 1D digital twin of the PHOENICE engine, developed in the commercial software GT-Suite [19], to support the calibration of the first engine prototype. First, a preliminary set of experimental data measured at 3000 RPM and 7 bar BMEP, including both EGR and λ variations, was used to assess the predictive capabilities of the combustion model. Afterwards, the developed virtual test rig was exploited to perform a calibration of the engine in terms of optimal λ and EGR combinations and, by way of examples, the results obtained for two engine operating points, a low load 1500 RPM and 5.5 bar BMEP and a high load 3000 RPM and 13 bar BMEP, will be presented and discussed.

The paper is organized as follow: first, additional details about the PHOENICE engine concept are provided, to then move to the virtual test rig development and its calibration, with particular attention to its phenomenological combustion model. Finally, the results obtained for the optimization of the mixture enleanment and EGR dilution are analyzed and discussed providing some hints for the future steps of the project.

THE PHOENICE ENGINE CONCEPT

The PHOENICE engine concept is based on a state-of-the-art 4-cylinder 1.3L turbocharged Direct Injection Spark Ignition (DISI) engine [20]. The former inherits from the latter an all-aluminum engine structure featuring a high stroke to bore ratio, a compact 4-valve combustion chamber with high pressure side fuel injectors, a MultiAir VVA system [21] and a cylinder head with integrated exhaust manifold. As part of the PHOENICE project, the baseline engine hardware has been upgraded with the technologies mentioned in the paper introduction and outlined in [Figure 1](#), with the goal of minimizing fuel consumption and pollutant emissions across the entire engine map while also taking advantage of the potentialities offered by powertrain hybridization.

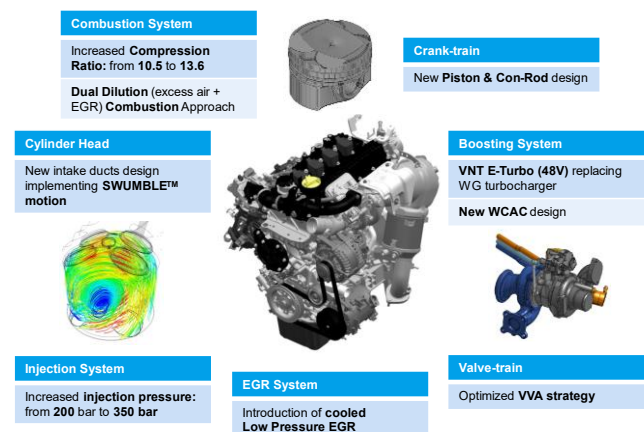


Figure 1: PHOENICE engine features

First, the piston has been redesigned to increase the Compression Ratio (CR) up to 13.6 and to enable lean

burn operation thanks to a Dual Dilution Combustion Approach (DDCA) which synergically exploits excess air and cooled low pressure EGR. The fuel injection system has been upgraded and it is now able to reach an injection pressure of 350 bar to support the ultra-lean combustion approach. Furthermore, the intake ducts and ports geometries have been optimized to implement the Swumble™, a newly developed charge motion concept able to consistently improve turbulence intensity by combining swirl and tumble in-cylinder motions with valuable effects on flame propagation [22, 23]. On the charging system side, a 48V electrified turbocharger embedding a Variable Nozzle Turbine (VNT) replaced the baseline Wastegate (WG) turbocharger. Its specifications were optimized in a previous work of the authors [24] to be compliant with the requirements of highly diluted mixtures and aggressive Miller cycle. Finally, the fully variable MultiAir valve actuation system, already integrated in the base engine configuration, enables Miller cycle exploitation through Early Intake Valve Closing (EIVC) or Late Intake Valve Closing (LIVC). The combination of all these technologies leads to the engine specifications summarized in [Table 3](#).

Table 3: PHOENICE engine specifications

Specification	Value
N. of Cylinders	4 in-line
Displacement	1332 cm ³
Bore x Stroke	Ø 70 mm x 86.5 mm
Stroke/Bore	1.24
Compression Ratio	13.6:1
Number of Valves	16
VVA System	MultiAir II (intake only)
Fuel Injection System	GDI
Turbocharging	VNT E-Turbo
Fuel	E10 (RON 97.3)
Rated Power (target)	100 kW @ 4500 RPM
Rated Torque (target)	218 Nm @ 3500 RPM

NUMERICAL MODEL DESCRIPTION AND VALIDATION

MODEL DESCRIPTION

A digital twin of the PHOENICE engine was developed in the commercially available software GT-Suite, a One-Dimensional Computational Fluid Dynamics (1D-CFD) code developed by Gamma Technologies [19]. The key aspect of the virtual test rig is the predictive combustion model, the SITurb [25, 26], through which it is possible to achieve a reliable estimation of the burn rate over a wide range of Air-Fuel Ratios (AFRs), EGR rates and valve timings. It relies on a two-zone approach in which the

combustion chamber is subdivided into burned and unburned gas regions. The turbulent propagating flame is modelled via a spherical propagation and with a typical entrainment and burn-up approach where the entrained mass (M_e) rate of the unburned air-fuel mixture in the flame front is dependent on the flame area (A_f), the unburned gas density (ρ_u), and the sum of the turbulent and laminar flame speeds (S_T and S_L , respectively) [27], as expressed by [Equation 1](#):

$$\frac{dM_e}{dt} = \rho_u \cdot A_f \cdot (S_T + S_L) \quad (1)$$

The model can be tuned through two calibration parameters, the turbulent flame speed multiplier (C_s), which globally scales the turbulent flame speed, and the flame kernel growth multiplier (C_k), which scales the flame front evolution. Both are included in the formulation of the turbulent flame speed S_T depicted in [Equation 2](#) in which R_f , u' and L_t refer to flame radius, turbulent intensity and turbulent length scale, respectively.

$$S_T = C_s \cdot u' \cdot \left(1 - \frac{1}{1 + \frac{C_k \cdot R_f^2}{L_t^2}} \right) \quad (2)$$

The laminar flame speed, instead, is computed through a mathematical formulation already available in the software (see [Equation 3](#)) and depending on the equivalence ratio ϕ , on the temperature of the unburned gases T_u , on the in-cylinder pressure p , and on the mass fraction of diluents D_i . This model also includes some constant (B_m , B_ϕ , ϕ_m , T_0 , ρ_0 , α and β) and a further calibration parameter, i.e., the dilution effect multiplier (C_D), which can be used to weight the effect of diluents such as exhaust residuals or EGR.

$$S_L = (B_m + B_\phi \cdot (\phi - \phi_m)^2) \cdot \left(\frac{T_u}{T_0} \right)^\alpha \cdot \left(\frac{p}{p_0} \right)^\beta \cdot \dots \cdot (1 - 0.75 \cdot C_D) \cdot (1 - (1 - 0.75 \cdot C_D \cdot [D_i]^7)) \quad (3)$$

Finally, [Equation 4](#) is used to determine the burn rate of the entrained unburned mass M_u :

$$\frac{dM_b}{dt} = \frac{M_u}{\tau} = \frac{M_e - M_b}{\tau} \quad (4)$$

where τ is assumed to be the time needed by the laminar flame speed to cover the Taylor microscale (λ) of turbulence, expressed by [Equation 5](#). The Taylor length scale multiplier C_λ , is a further calibration parameter inversely proportional to the burn-up rate:

$$\tau = \frac{\lambda \cdot C_\lambda}{S_L} \quad (5)$$

For the optimization of the PHOENICE concept, a reliable knock model is mandatory. In 1D-CFD codes

the knock prediction usually relies on the Livengood and Wu approach, which assumes that the auto-ignition of the end gas occurs when:

$$\int_{t=0}^{t_{\text{knock}}} \frac{1}{T} dt = 1 \quad (6)$$

where τ is the knock induction time of the air-fuel mixture and t_{knock} is the time corresponding to the auto-ignition instant (computed from the start of compression). To calculate the knock induction time, phenomenological formulas developed for gasoline mixture are typically employed [28, 29]. The Kinetics-Fit model, proposed by Gamma Technologies, [19], was chosen among them because, unlike the well-known Douad-Eyzat [30], it considers the dependence of the knock induction time on the mixture composition in terms of diluents (such as EGR), and it can replicate the Negative Temperature Coefficient (NTC) behavior [31, 32] as described by [Equation 7](#).

$$\tau = \mathbf{KITM} \cdot a_i \cdot \left(\frac{\text{RON}}{100}\right)^{b_i} \cdot [\text{Fuel}]^{c_i} \cdot [\text{O}_2]^{d_i} \cdot [\text{D}_i]^{e_i} \cdot \dots \cdot \exp\left(\frac{f_i}{\mathbf{AEM} \cdot T_u}\right) \quad (7)$$

The model also considers the fuel knock resistance through the Research Octane Number (RON), the unburned gas temperature T_u , the reactants ([Fuel] and $[\text{O}_2]$) and diluent ($[\text{D}_i]$) concentrations. The latter is calculated as the sum of N_2 , CO_2 , and H_2O . Finally, quantities from a_i to f_i are model constants.

MODEL CALIBRATION AND VALIDATION

The combustion model described in the previous section was initially calibrated by the authors in a previous work by using a preliminary set of experimental data collected on an engine prototype that still retained the baseline turbocharger and exhaust line [33]. The model was then improved using additional measurements taken on an updated version of the engine prototype that includes all the PHOENICE contents. In particular, the dilution effect multiplier (see [Equation 3](#)) was adjusted on the basis of an experimental investigation carried out at 3000 RPM and 7 bar BMEP to better capture the sensitivity of the combustion process to the exploitation of higher dilution rates. This investigation involved an EGR sweep for four different λ setpoints ranging from stoichiometric up to lean conditions. The considered EGR rates for each λ value are shown in [Figure 2](#).

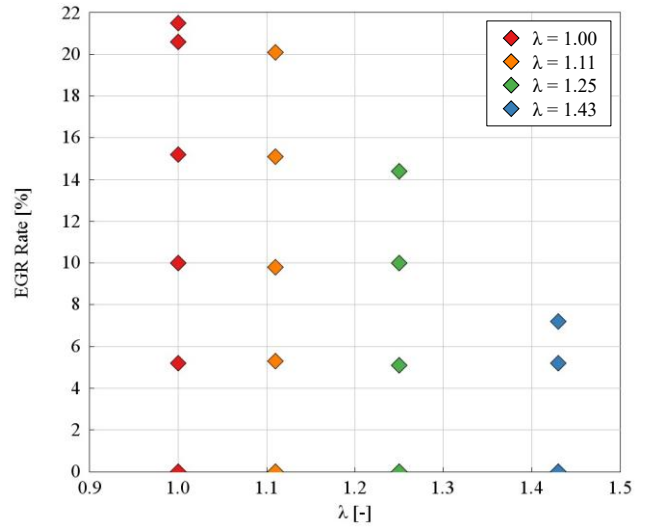


Figure 2: Experimental investigation of dual dilution combustion at 3000 RPM and 7 bar BMEP. EGR rate sweeps for different λ setpoints

As it can be observed in [Figure 3](#), a good agreement between simulations and experimental tests was achieved. Imposing the experimental spark advance in the model, the correlation plot of the combustion center of gravity ([Figure 3.a](#)) showed a maximum error of about 2 CAD while the simulated burn duration deviated from the measurements only with very slow combustion which corresponds to EGR rates larger than 20% ([Figure 3.b](#)).

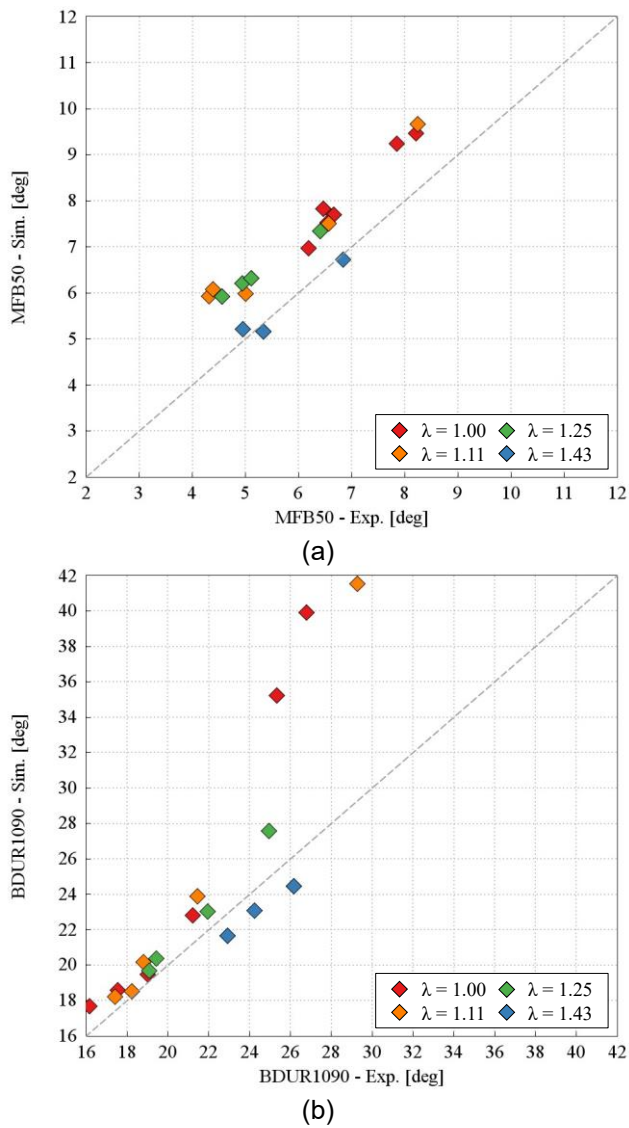


Figure 3: Correlation Plot at different λ and EGR Rate. – (a): Combustion Center of Gravity – (b): Burn Duration 10-90

According to this behavior, burn rates and pressure traces can be accurately predicted under a variety of operating conditions, as shown in Figure 4 where a λ variation is reported for a moderate EGR rate of about 10% for $\lambda = 1.00, 1.11$ and 1.23 and 7% for $\lambda=1.43$.

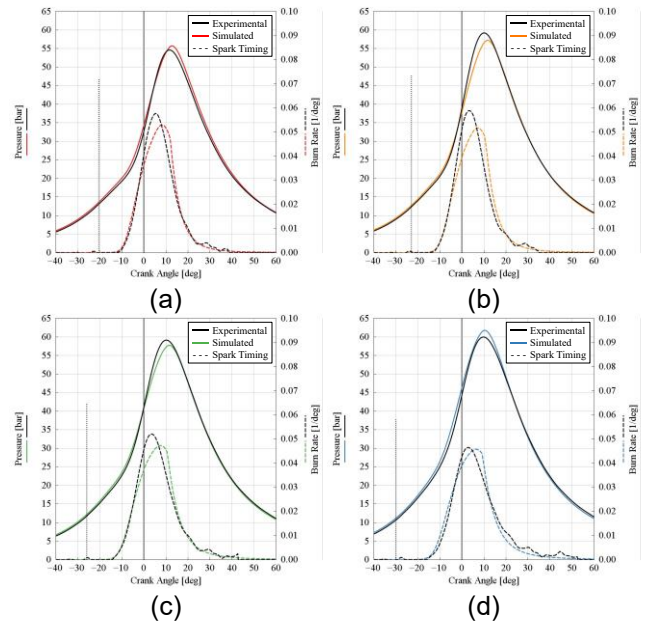


Figure 4: Comparison between the simulated and measured pressure traces and burn rates at moderate EGR rate. – (a): $\lambda = 1$ – (b): $\lambda = 1.11$ – (c): $\lambda = 1.25$ – (d): $\lambda = 1.43$

To prove the robustness of the proposed calibration, an additional comparison was performed at 3000 RPM and 13 bar BMEP with a stoichiometric λ and considering different EGR levels (5% – 10% – 15% – 20%).

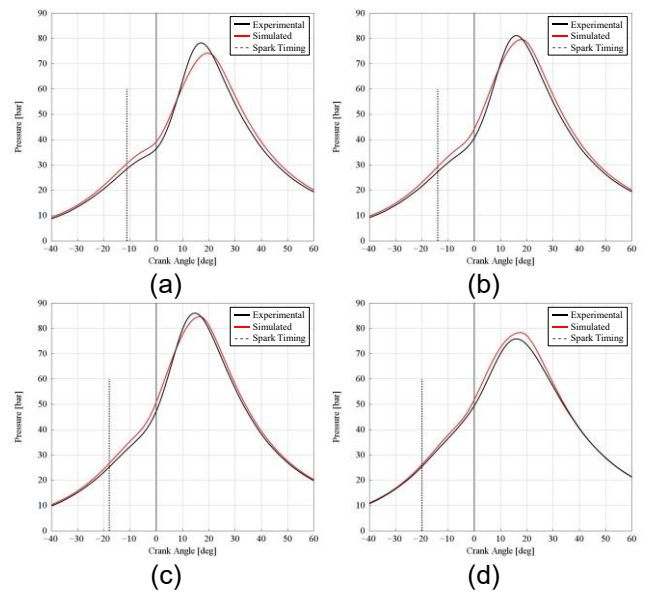


Figure 5: Comparison between the simulated and measured pressure traces at different EGR rate. – (a): EGR=5% – (b): EGR=10% – (c): EGR=15% – (d): EGR=20%

Figure 5, which shows the in-cylinder pressure traces in the considered operating conditions, points out a very good matching between the simulations and the experimental measurements. The maximum deviation can be observed with an EGR rate of 5% where the peak pressure is underestimated of about 4 bar.

VIRTUAL CALIBRATION

Once the predictive combustion model had been calibrated and tested with satisfactory correlation results, the developed virtual test rig was used to identify the optimal combination of air/fuel ratios and EGR rates leading to the maximum engine thermal efficiency, thus further improving the first calibration maps previously defined by the authors in [33]. For sake of brevity, only the results obtained for the two engine operating points shown in Figure 6 (a low load point corresponding to 1500 RPM and 5.5 bar BMEP and a high load point corresponding to 3000 RPM and 13 bar BMEP) will be discussed hereafter.

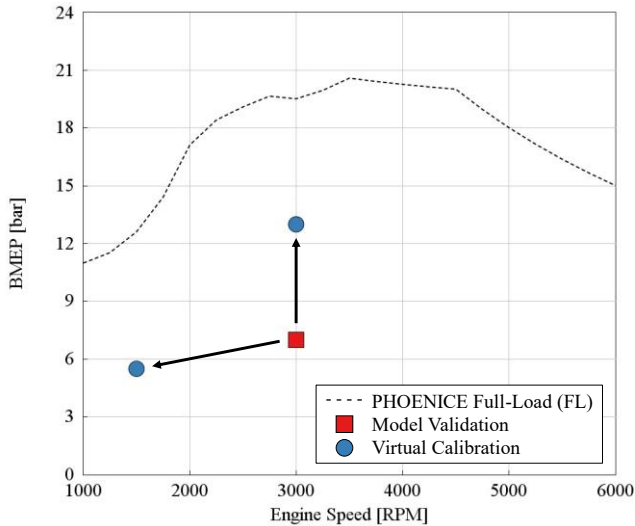


Figure 6: Engine operating points selected for model validation (red square) and virtual calibration (blue circles)

For each of the two engine key points, a full factorial Design of Experiment (DoE) approach was adopted. Four different λ values, i.e., 1.0 – 1.2 – 1.4 – 1.6, together with four different levels of EGR rates, i.e., 0% – 5% – 10% – 15%, were tested. The corresponding test matrix is depicted in Figure 7.

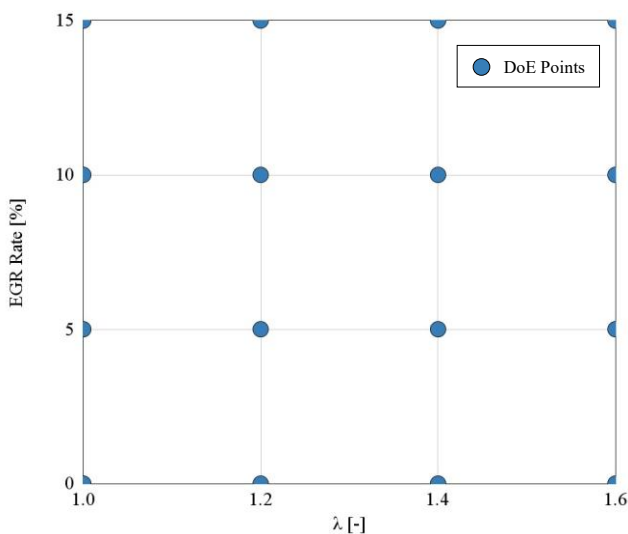


Figure 7: DoE test matrix for Virtual Calibration

HIGH LOAD POINT

In this paragraph the findings regarding the high load operating point (3000 RPM and 13 bar BMEP) are discussed. The virtual engine was run at Knock

Limited Spark Advance (KLSA) and with the intake and exhaust valve lifts and timings shown in Figure 8.

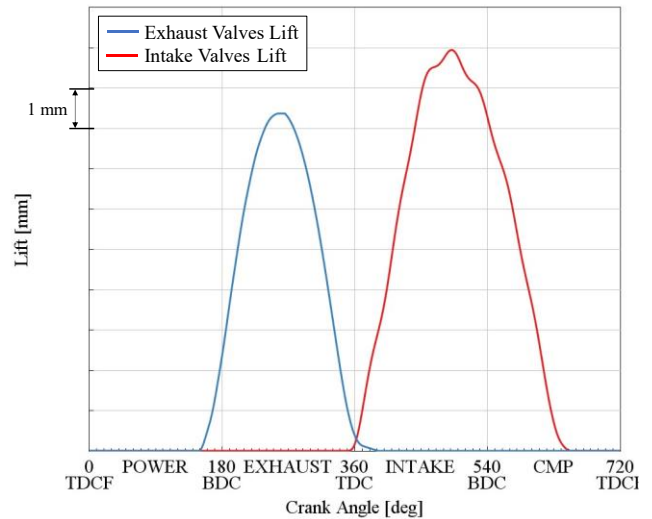


Figure 8: 3000 RPM and 13 bar BMEP. Intake and exhaust valve lifts

The results obtained through the DoE investigation are reported in Figure 9. The highest indicated efficiency (identified by the star marker) is obtained when the engine is operated at moderately diluted mixture with $\lambda = 1.2$ and with 5% EGR. As a matter of fact, this combination of λ and EGR represents the best tradeoff between knock suppression, pumping losses and combustion duration. Indeed, higher air/fuel ratios or EGR rates could further improve the combustion phasing thanks to the lower knock tendency, but, on the contrary, would increase both the backpressure, because of the higher boost requirements, and the combustion duration.

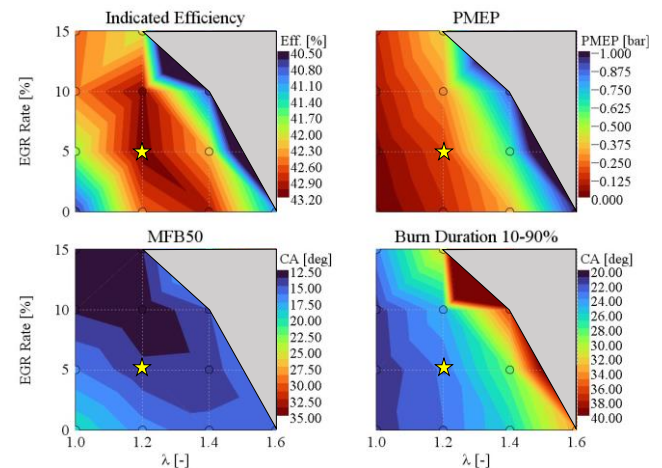


Figure 9: 3000 RPM and 13 bar BMEP. Virtual Calibration results

LOW LOAD POINT

In this paragraph the findings regarding the low load operating point (1500 RPM and 5.5 bar BMEP) are discussed. The virtual engine was run at Maximum Brake Torque (MBT) spark timing (corresponding to an MFB50 of about 8 CAD aTDCf) and with the intake and exhaust valve lifts and timings shown in Figure 10.

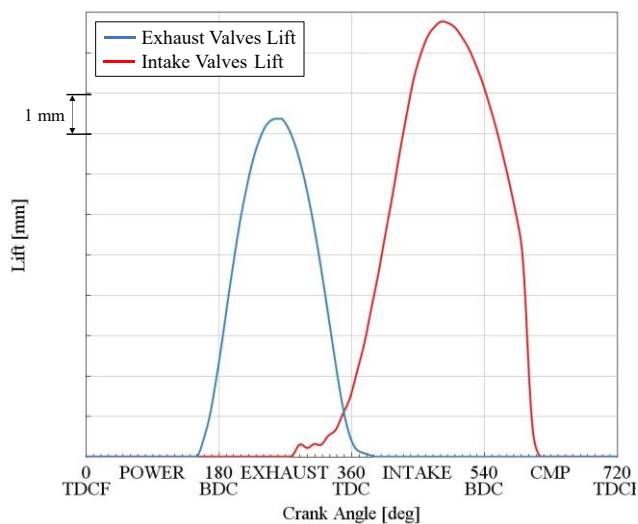


Figure 10: 1500 RPM and 5.5 bar BMEP. Intake and exhaust valve lifts

The results obtained through the DoE investigation are reported in [Figure 11](#). The highest indicated efficiency (identified by the star marker) is obtained when the engine is operated with a significant enleanment ($\lambda = 1.4$) and with a moderate EGR rate equal to 5%. As a matter of fact, this combination of λ and EGR proved to be the most effective in exploiting de-throttling to achieve the lowest pumping work while maintaining an acceptable combustion duration. On the other hand, a further increase of either the EGR rate or the air/fuel ratio could produce a significant deterioration of the combustion process which would jeopardize the benefits due to the additional reduction of the PMEP.

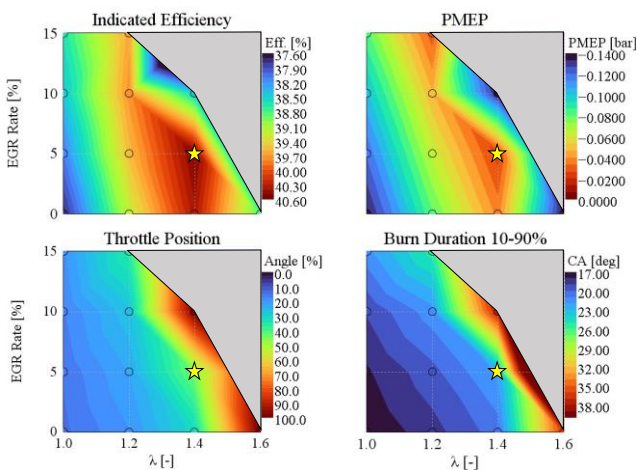


Figure 11: 1500 RPM and 5.5 bar BMEP. Virtual Calibration results

CONCLUSION

In this paper, a 1D engine model was developed to support the calibration of the innovative highly efficient spark ignition engine of the PHOENICE EU H2020 project, by synergistically exploiting the combination of innovative in-cylinder charge motion, Miller cycle with high compression ratio, lean mixture with cooled EGR and electrified turbocharger. To fully exploit the potential of mixture enleanment and dilution with cooled EGR, particular attention was devoted to the definition of a reliable combustion model to properly

predict the burn duration and the occurrence of abnormal combustion phenomena. After a preliminary calibration of the model performed on a set of experimental data measured at 3000 RPM and 7 bar BMEP, including both EGR and λ sweeps, the developed virtual test rig was then exploited to perform a calibration of the engine in terms of optimal λ and EGR combinations. As an example, the results obtained at two different engine operating points, a low load 1500 RPM and 5.5 bar BMEP and a high load 3000 RPM and 13 bar BMEP, were presented and discussed in this paper. Results showed that the best efficiency values, well above 40% indicated efficiency, could be obtained with moderate dilution and EGR rates. As a matter of fact, these calibrations allowed to achieve the optimal trade-off between the increased combustion duration and the improved combustion phasing thanks to knock suppression at high load. On the other hand, at low load the optimal combination between mixture enleanment and EGR dilution allowed to achieve the best trade-off between the increased combustion duration and the reduced pumping work thanks to de-throttling. Future steps will focus on the integration of after-treatment models in the virtual test rig to predict tailpipe emissions. Moreover, transient simulations will be performed to assess the achievement of the project targets in both regulatory and real-world driving conditions.

ACKNOWLEDGMENTS

This project has received funding from the European Union's Horizon 2020 research and innovation program under Grant Agreement No. 101006841.

REFERENCES

1. Dornoff, J., Mock, P., Baldino, C., Bieker, G. et al., "Fit for 55: A review and evaluation of the European Commission proposal for amending the CO2 targets for new cars and vans," ICCT Briefing, 2021.
2. Kramer, U., Bothe, D., Gatzen, C., Pfannenschmidt, A. et al., "Transformation of Mobility to the GHG-Neutral Post-Fossil Age," FVV Fuel Study IV, 2022.
3. Tahtouh, T., Brignone, M., Cleeton, J., Demeilliers, N. et al., "PHEV towards zero Emission & ultimate ICE efficiency: the PHOENICE project," in CO2 reduction for Transportation Systems Conference, Turin, 21-22 June 2022.
4. Samaras, Z., Kontses, A., Dimaratos, A., Kontses, D. et al., "A European Regulatory Perspective towards a Euro 7 Proposal," SAE Technical Paper 2022-37-0032, 2022, <https://doi.org/10.4271/2022-37-0032>.
5. Yang, D., Lu, G., Gong, Z., Qiu, A. et al., "Development of 43% Brake Thermal Efficiency Gasoline Engine for BYD DM-i Plug-in Hybrid," SAE Technical Paper 2021-01-1241, 2021, <https://doi.org/10.4271/2021-01-1241>.
6. Osborne, R., Lane, A., Turner, N., Geddes, J. et al., "A New Generation Lean Gasoline Engine for Premium Vehicle CO2 Reduction," SAE Technical Paper 2021-01-0637, 2021,

- <https://doi.org/10.4271/2021-01-0637>.
7. Bunce, M., Peters, N., Pothuraju Subramanyam, S., Blaxill, H. et al., "The Impact of Advanced Fuels and Lubricants on Thermal Efficiency in a Highly Dilute Engine," *SAE Int. J. Adv. & Curr. Prac. in Mobility* 3(5):2540-2553, 2021, <https://doi.org/10.4271/2021-01-0462>.
 8. Bisws, S., "Physics of Turbulent Jet Ignition," Springer Cham, 2018, <https://doi.org/10.1007/978-3-319-76243-2>.
 9. Lee, K., Bae, C., and Kang, K., "The effects of tumble and swirl flows on flame propagation in a four-valve S.I. engine," *Applied Thermal Engineering* 27(11–12):2122–2130, 2007, <https://doi.org/10.1016/j.applthermaleng.2006.11.011>.
 10. Scarcelli, R., Matthias, N., and Wallner, T., "Numerical Investigation of Combustion in a Lean Burn Gasoline Engine," SAE Technical Paper 2013-24-0029, 2013, <https://doi.org/10.4271/2013-24-0029>.
 11. Kumano, K. and Yamaoka, S., "Analysis of Knocking Suppression Effect of Cooled EGR in Turbo-Charged Gasoline Engine," SAE Technical Paper 2014-01-1217, 2014, <https://doi.org/10.4271/2014-01-1217>.
 12. Francqueville, L. and Michel, J., "On the Effects of EGR on Spark-Ignited Gasoline Combustion at High Load," *SAE Int. J. Engines* 7(4):1808-1823, 2014, <https://doi.org/10.4271/2014-01-2628>.
 13. Potteau, S., Lutz, P., Leroux, S., Moroz, S. et al., "Cooled EGR for a Turbo SI Engine to Reduce Knocking and Fuel Consumption," SAE Technical Paper 2007-01-3978, 2007, <https://doi.org/10.4271/2007-01-3978>.
 14. Millo, F., Luisi, S., Borean, F., and Stroppiana, A., "Numerical and experimental investigation on combustion characteristics of a spark ignition engine with an early intake valve closing load control," *Fuel* 121:298–310, 2014, <https://doi.org/10.1016/j.fuel.2013.12.047>.
 15. Luisi, S., Doria, V., Stroppiana, A., Millo, F. et al., "Experimental Investigation on Early and Late Intake Valve Closures for Knock Mitigation through Miller Cycle in a Downsized Turbocharged Engine," SAE Technical Paper 2015-01-0760, 2015, <https://doi.org/10.4271/2015-01-0760>.
 16. Davies, P., Bontemps, N., Tietze, T. and Faulseit, E., "Electric Turbocharging - Key Technology for Hybridized Powertrains," *MTZ Worldw* 80:30-37, 2019, <https://doi.org/10.1007/s38313-019-0096-y>.
 17. Cooper, A., Reader, S., Bassett, M., Hall, et al., "HyPACE-Hybrid Petrol Advanced Combustion Engine," in 27th Aachen Colloquium Automobile and Engine Technology, Aachen, 8-10 October 2018.
 18. Boccardo, G., Piano, A., Zanelli, A., Babbi, M., et al., "Development of a virtual methodology based on physical and data-driven models to optimize engine calibration," *Transportation. Engineering.* 10 (2022) 100143, 2022, <https://doi.org/10.1016/j.treng.2022.100143>.
 19. GT-SUITE Engine Performance Application Manual, Software User Manual; Gamma Technologies: Westmont, IL, USA, 2022.
 20. De Marino, C., Maiorana, G., Pallotti, P., Quinto, S. et al., "The Global Small Engine 3 and 4 Cylinder Turbo: The New FCA's Family of Small High-Tech Gasoline Engines," in 39th International Vienna Motor Symposium, Vienna, 26-27 April 2018.
 21. Bernard, L., Ferrari, A., Micelli, D., Peretto, A. et al., "Electro-hydraulic Valve Control with MultiAir Technology," *MTZ Worldw* 70:4-10, 2009, <https://doi.org/10.1007/BF03226988>.
 22. Bourhis, G., Laget, O., Kumar, R. and Gautrot, X., "Swumble In-Cylinder Fluid Motion: a Pathway to High Efficiency Gasoline SI Engines," in 27th Aachen Colloquium Automobile and Engine Technology, Aachen, 8-10 October 2018.
 23. Gautrot, X., Bardi, M., Leroy, T., Luca, P. et al., "SwumbleTM In-Cylinder Fluid Motion for High Efficiency Gasoline SI Engines: development of the second generation," in Proceedings of the SIA Powertrain and Electronics, Rouen, 16-29 November 2020.
 24. Tahtouh, T., Millo, F., Rolando, L., Castellano, G. et al. "A Synergic Use of Innovative Technologies for the Next Generation of High Efficiency Internal Combustion Engines for PHEVs: the PHOENICE Project," SAE Technical Paper 2023-01-0224, 2023, <https://doi.org/10.4271/2023-01-0224>.
 25. Mirzaeian, M., Millo, F., and Rolando, L., "Assessment of the Predictive Capabilities of a Combustion Model for a Modern Downsized Turbocharged SI Engine," SAE Technical Paper 2016-01-0557, 2016, <https://doi.org/10.4271/2016-01-0557>.
 26. Millo, F., Gullino, F., and Rolando, L., "Methodological approach for 1D simulation of port water injection for knock mitigation in a turbocharged DISI engine," *Energies (Basel)* 13(17), 2020, <https://doi.org/10.3390/en13174297>.
 27. Wahiduzzaman, S., Moral, T., and Sheard, S., "Comparison of Measured and Predicted Combustion Characteristics of a Four-Valve S.I. Engine," SAE Technical Paper 930613, 1993, <https://doi.org/10.4271/930613>.
 28. By, A., Kempinski, B., and Rife, J., "Knock in Spark Ignition Engines," SAE Technical Paper 810147, 1981, <https://doi.org/10.4271/810147>.
 29. Belli, M., Danieli, G., Amelio, M., Bova, S. et al., "A Detonation Model in Spark-Ignition Engines: Preliminary Results on Engine Octane Requirement," SAE Technical Paper, 1984.
 30. Douaud, A. and Eyzat, P., "Four-Octane-Number Method for Predicting the Anti-Knock Behavior of Fuels and Engines," SAE Technical Paper, 1978.
 31. Hahn, T., "Ignition Study in Rapid Compression Machine," Bachelor's Thesis, MIT, Cambridge, MA, USA, 2006.
 32. Schernus, C., Nebbia, C., Di Matteo, F., Thewes, M., "Application of the New Kinetic Knock Model to A Downsized TGDI Engine," in Proceedings of the Gamma Technology User Conference 2013, Frankfurt, 21–22 October

2013.
33. Tahtouh, T., Andre, M., Millo, F., Rolando, L. et al., "Development of a Digital Twin to Support the Calibration of a Highly Efficient Spark Ignition Engine," SAE Technical Paper 2023-01-1215, 2023, <https://doi.org/10.4271/2023-01-1215>.

CONTACT

Dr. Toni Tahtouh
IFP Energies Nouvelles - Mobility and Systems
Division
1 et 4 avenue de Bois-Préau
92852 Rueil-Malmaison Cedex – France
toni.tahtouh@ifpen.fr.

DEFINITIONS, ACRONYMS, ABBREVIATIONS

1D-CFD: One-Dimensional Computational Fluid Dynamics

AEM: Activation Energy Multiplier

AFR: Air-to-Fuel Ratios

BMEP: Brake Mean Effective Pressure

CAD aTDCf: Crank Angle Degrees after Top Dead Center of firing

CR: Compression Ratio

DDCA: Dual Dilution Combustion Approach

DISI: Direct Injection Spark Ignition

DoE: Design of Experiments

EGR: Exhaust Gas Recirculation

EIVC: Early Intake Valve Closing

GDI: Gasoline Direct Injection

GHG: Green House Gases

ICE: Internal Combustion Engine

IMEP: Indicated Mean Effective Pressure

KITM: Knock Induction Time Multiplier

KLSA: Knock-Limited Spark Advance

LIVC: Late Intake Valve Closing

MBT: Maximum Brake Torque

MFB50: Crank angle corresponding to 50% of fuel Mass Fraction Burned over an engine cycle

NTC: Negative Temperature Coefficient

PHEV: Plug-in Hybrid Electric Vehicle

PMEP: Pumping Mean Effective Pressure

RON: Research Octane Number

RPM: Revolutions Per Minute

TJI: Turbulent Jet Ignition

VNT: Variable Nozzle Turbine

VVA: Variable Valve Actuation

WG: Wastegate

SYMBOLS

A_f: Flame Area

C_D: Dilution Effect Multiplier

C_k: Flame Kernel Development Multiplier

C_s: Turbulent Flame Speed Multiplier

C_λ: Taylor Length Multiplier

D_i: Mass Fraction of Diluents in the Unburned Zone

L_t: Turbulent Length Scale

M_b: Burned Mass

M_e: Entrained Mass

M_u: Unburned Mass

p: In-cylinder Pressure

R_f: Flame Radius

S_L: Laminar Flame Speed

S_T: Turbulent Flame Speed

T_u: Unburned Gas Temperature

u': Turbulence intensity

λ: Taylor microscale

ρ_u: Unburned Gas Density

τ: Knock Induction Time

φ: Equivalence Ratio